www.czasopisma.pan.pl www.journals.pan.pl
Chemical and Process Engineering 2014, 35 (3), 331-348
DOI: 10.2478/cpe-2014-0025

MODELLING OF THE BUBBLE SIZE DISTRIBUTION IN AN AERATED STIRRED TANK: THEORETICAL AND NUMERICAL COMPARISON OF DIFFERENT BREAKUP MODELS

Zbyněk Kálal*[1], Milan Jahoda[1], Ivan Fořt[2]

[1]Institute of Chemical Technology, Prague, Technická 5, 166 28 Prague 6, Czech Republic

[2]Czech Technical University in Prague, Technická 4, 166 07 Prague 6, Czech Republic

The main topic of this study is the mathematical modelling of bubble size distributions in an aerated stirred tank using the population balance method. The air-water system consisted of a fully baffled vessel with a diameter of 0.29 m, which was equipped with a six-bladed Rushton turbine. The secondary phase was introduced through a ring sparger situated under the impeller. Calculations were performed with the CFD software CFX 14.5. The turbulent quantities were predicted using the standard k-ε turbulence model. Coalescence and breakup of bubbles were modelled using the MUSIG method with 24 bubble size groups. For the bubble size distribution modelling, the breakup model by Luo and Svendsen (1996) typically has been used in the past. However, this breakup model was thoroughly reviewed and its practical applicability was questioned. Therefore, three different breakup models by Martínez-Bazán et al. (1999a, b), Lehr et al. (2002) and Alopaeus et al. (2002) were implemented in the CFD solver and applied to the system. The resulting Sauter mean diameters and local bubble size distributions were compared with experimental data.

Keywords: CFD, mixing, gas-liquid, population balance, bubble breakup

1. INTRODUCTION

A particle size distribution in the secondary phase (bubbles, droplets and solid particles) exists in many industrial applications, e.g., crystallisation, granulation, fluid polymerisation or aerobic fermentation in bubble columns and stirred tanks. The change in the particle size can be caused by a combination of various phenomena such as nucleation, growth, dissolution, aggregation or breakup. To capture this process, an additional equation that describes changes in the particle size distribution must be solved together with other transport equations for multiphase flow. This equation is generally referred to as the population balance equation (PBE, see Eq.(3)).

A constant size of the dispersed phase is often assumed in the mathematical modelling of gas-liquid systems because the employment of the bubble size distribution (BSD) modelling significantly increases the computational time. However, this idea does not capture the real situation because coalescence and breakup occur via bubble-bubble and bubble-liquid interactions. Gas-liquid systems may thus exhibit high inhomogeneity in the BSD. Therefore, the constant bubble size model cannot correctly describe the interfacial forces, gas hold-up or mass and heat transfer between phases, which are generally functions of bubble size. This issue was first addressed by Bakker and van den Akker (1994). They introduced a single equation for the bubble number density. The mean bubble diameter at

*Corresponding author, e-mail: kalalz@vscht.cz

each point throughout the domain is calculated from the computed local bubble number density and gas hold-up. This approach is computationally undemanding; however, the distribution of bubble sizes is not resolved.

To determine the BSD, it is necessary to solve the PBE that describes the bubble population evolution. It is a complicated integro-partial differential equation. As a consequence, it is only possible to solve it analytically in rare cases, and we usually have to resort to various numerical methods to address it. A group of these methods, the class methods (CM), are based on the discretisation of the continuous size range of the particle population to a finite number of size intervals (called classes, groups or bins). A transport equation must be solved for each interval. Every group is represented by a specific value for the particle size, and each particle can interact with particles in other groups. Vanni (2000) compared various solution procedures that had been proposed for the CM. The most robust and versatile is the fixed pivot technique developed by Kumar and Ramkrishna (1996). The main drawback of this technique is that it contains the integration of the daughter size distribution (DSD) function of the breakup model. If the DSD function itself includes an integral, the resulting source terms in the PBE may contain a double or even a triple integral, which significantly complicates the method of computation. In addition, some DSD functions present a stiff behaviour and so integration methods with a high number of nodes or adaptive integration methods are needed. Lo (1996) proposed a similar method and called it the Multiple Size Group (MUSIG) method. It uses the partial breakup rates instead of the overall breakup rates and so avoids the integration of the DSD function, which makes the use of the method more feasible.

The CM are especially used in cases when the sizes of the largest and the smallest particles are known, and this range is not too big so that we can discretise the population with a relatively small number of intervals. The main advantage of this approach is the direct computation of the BSD, but at the expense of increased computational demands. The alternatives to the CM are the methods of moments, where the BSD is not tracked directly but is tracked through its moments. The PBE is transformed into a set of transport equations for the individual moments of the distribution. Generally, it is sufficient to solve two to six moment equations, and so a lower number of equations is needed in comparison with the CM and the computational time is spared. However, the BSD is not directly accessible and must be reconstructed from the computed moments. The basic Standard Method of Moments (SMOM) was quickly abandoned because the exact closure to the right-hand side of the PBE is not possible except for some special cases as, e.g., the constant aggregation rate and no breakup.

To overcome the closure problem, the SMOM was modified. The moments were described via quadratic approximation, which eliminated problems with particle coalescence and breakage descriptions. The weights and nodes of the quadrature approximation are calculated using a proper algorithm, e.g., the product-difference algorithm (Gordon, 1968). This has given rise to the Quadrature Method of Moments (QMOM) (Marchisio and Fox, 2013; McGraw, 1997). The standard QMOM is able to resolve only monodimensional systems (i.e., systems with one internal coordinate, typically size). To extend to the multidimensional problems, the direct QMOM, in which the weights and nodes are calculated directly from the transport equations (Marchisio and Fox, 2005), and the conditional QMOM, in which the weights and nodes are computed by resorting to a different algorithm (Yuan and Fox, 2011), have been derived.

Both the CM and the QMOM are able to address the PBE and provide correct results (Selma et al., 2010). The essential factor is rather the selection of the appropriate coalescence and breakup models. While the coalescence models usually exhibit similar behaviours, various breakup models significantly differ in the predicted breakup frequencies or in the shapes of the DSD functions. It is not absolutely clear which of the models accurately represents realistic behaviour as evidenced by the published experimental results on bubble breakup, which are sometimes contradictory. Hesketh et al. (1991) and Andersson and Andersson (2006) claim that binary breakup is the most probable event for bubble breakup, while Risso and Fabre (1998) observed breakups that formed more than ten fragments.

Although some earlier works considered equal-sized breakage as the most probable outcome, Hesketh's and Andersson's works support the fact that the unequal-sized breakage is dominant for bubbles. This is in agreement with the theoretical consideration that the unequal-sized breakup should be energetically less demanding than the equal-sized breakup and is thereby more probable. The most frequently used breakup model was derived by Luo and Svendsen (1996). It has been applied by many authors for modelling the BSD in stirred tanks (e.g., Ahmed et al., 2010; Kerdouss et al., 2008; Montante et al., 2008; Ranganathan and Sivaraman, 2011; Selma et al., 2010); other models have seldom been applied (Gimbun et al., 2009; Laakkonen et al., 2007). The model by Luo & Svendsen was introduced in our previous work (Kálal et al., 2014). This paper further explores the model's features and compares it with other breakup models.

The importance of an accurate gas hold-up prediction should be mentioned because coalescence and breakup rates are related to it. The measurement of global gas hold-up is quite simple and is based on the liquid height elevation. This parameter is thus usually respected in CFD simulations of multiphase stirred tanks and the simulated values are compared with the experimental ones. However, a correct prediction of the global gas hold-up does not ensure that the local gas hold-up is modelled correctly as well. The critical issue is that the measurement of local gas hold-up is more complicated and requires sophisticated equipment. Therefore, there exists only limited amount of experimental data in the literature (Alves et al., 2002; Khopkar et al., 2005), and usually we have to resort to a comparison of numerical results with visual observations.

The breakup and coalescence kernels are strong functions of the turbulent dissipation energy. The correct prediction of turbulent quantities is thus essential for BSD modelling. Coroneo et al. (2011) tested four different computational grids ranging from 270,000 to 6.6 million cells and concluded that the turbulent quantities prediction may be significantly improved by reducing the spatial discretisation size, i.e., very fine grids are required for the correct prediction of turbulent field.

The objective of this article is to summarise the various breakup models provided in the literature and to present CFD simulations of the bubble size distributions in an aerated stirred tank. The resulting local Sauter mean diameters and local bubble size distributions computed via four different breakup models are presented and compared with experiments.

2. EXPERIMENTAL SETUP

Experiments were performed in a cylindrical, fully-baffled vessel with a diameter $T = 0.29$ m, which was filled with tap water to height T. The tank was equipped with a standard six-bladed Rushton turbine of diameter $T/3$, the distance of which from the vessel bottom was $T/3$. The turbine rotated with a constant speed of 300 rpm. A ring sparger was positioned halfway between the vessel bottom and the lower edge of the impeller. The sparger contained six point outlets with diameters of 1.5 mm through which air was introduced into the system. The volumetric gas flow rate was varied from 4 l/min to 8 l/min (0.2 and 0.4 vvm).

The determinations of both global gas hold-up and local BSDs were accomplished using photographic analysis. To prevent distortion of the view through a rounded wall, the mixing tank was placed in a rectangular, glass vessel filled with water. A set of lights was positioned on both sides of the tank and above the free liquid surface. These lights illuminated only the plane where bubble snapshots were taken so that the unwanted background was significantly suppressed, which facilitated the identification of bubbles situated in the plane. The captured bubbles were identified manually, and their size was evaluated via image analysis using the NIS-Elements software. A detailed description of the experimental techniques can be found in our previous work (Kálal et al., 2014).

3. GOVERNING EQUATIONS

In the Eulerian model, all phases are considered to be interpenetrating continua. The volume fraction and the velocity components of each phase are computed from the continuity equation and the Navier-Stokes equations, respectively. The velocity fluxes at the cell faces were obtained using the Rhie-Chow algorithm (Rhie and Chow, 1983). The gas distribution inside a tank is strongly influenced by a proper modelling of the interphase forces. The most significant interphase force in stirred tanks is the drag force (Scargiali et al., 2007), which is mathematically described via the drag coefficient. Based on our previous results (Kálal et al., 2014), we have chosen the drag coefficient description by Montante et al. (2007) as the most suitable for our simulation. It is simply expressed from the force balance applied to a particle:

$$c_D = \frac{4 g d_b \left(\rho_l - \rho_g\right)}{3 \rho_l U_t^2} \tag{1}$$

The critical factor of this expression is the bubble terminal rise velocity in a turbulent fluid U_t. We can find many correlations for the calculation of the bubble terminal rise velocity in stagnant fluids U_s (Clift et al., 1978; Mendelson, 1967). However, the rise velocity is significantly decreased in turbulent flows, and an exact description of the dependence of U_t on hydrodynamic variables is difficult to determine. Fajner et al. (2008) provided an expression for U_t in stirred tanks:

$$\frac{U_t}{U_s} = 0.32 \tanh\left(19 \frac{\eta}{d_b} \sqrt{\frac{\rho_l - \rho_g}{\rho_l}} - 1\right) + 0.6 \tag{2}$$

where η is the Kolmogorov microscale. The expression was derived for solid-liquid flow and so it cannot capture the increased drag due to bubble deformations, which resulted in underestimations of the drag in the impeller discharge stream. To the authors' knowledge, no correlation for computation of U_t in gas-liquid systems is presently available and the whole issue is far from being completely addressed both experimentally and numerically. Hence, a simplified approach that proved to be successful in our previous work was applied. It is based on two values of U_t for the high-turbulent and less-turbulent areas - 8 cm/s for $\varepsilon \geq 1.0$ m^2/s^3 and 13 cm/s for $\varepsilon < 1.0$ m^2/s^3 (Kálal et al., 2014).

The turbulent dispersion force was included in the model; other interaction forces were neglected.

3.1. Population balance model

The PBE defines how the population of particles develops over time. It is based on the number density function $n(\xi,t)$, which represents the number of particles per unit volume with values of a property ξ (usually size V) in the range ξ to ξ+dξ. If the growth and nucleation terms are neglected, the PBE can be written in terms of V as:

$$\frac{\partial}{\partial t}\left[n(V,t)\right] + \nabla \cdot \left[\vec{U}_g n(V,t)\right] = B_{ag}(V,t) - D_{ag}(V,t) + B_{br}(V,t) - D_{br}(V,t) \tag{3}$$

where $B_{ag}(V,t)$ and $B_{br}(V,t)$ express the birth rates of bubbles of size V to V+dV due to aggregation and breakup, respectively, and $D_{ag}(V,t)$ and $D_{br}(V,t)$ are the corresponding death rates.

To derive a system of equations for the CM, it is necessary to carry out some mathematical treatments. By integrating the PBE over a size interval we obtain its discretised form:

$$\frac{\partial n_i}{\partial t} + \nabla \cdot \left(\vec{U}_g n_i\right) = B_{ag,i} - D_{ag,i} + B_{br,i} - D_{br,i} \tag{4}$$

where n_i represents the number of bubbles of class i per unit volume. Multiplying by ρ_g and using the

relationship $\alpha_g \cdot f_i = n_i \cdot V_i$, we receive the discretised equation for class *i*:

$$\frac{\partial}{\partial t}\left(\alpha_g \rho_g f_i\right) + \nabla \cdot \left(\alpha_g \rho_g \vec{U}_g f_i\right) = B_{ag,i} - D_{ag,i} + B_{br,i} - D_{br,i} \tag{5}$$

where f_i is the volumetric fraction of class *i* in gas. The transported scalars that the discretised PBE is solved for are then the volumetric fractions of classes f_i instead of the number densities n_i. This modification is advantageous from the numerical point of view because the number densities generally take very large values which can lead to round-off errors during calculations.

The source terms can be written according to Lo (1996):

$$B_{ag,i} = \rho_g \alpha_g^2 \frac{1}{2} \sum_{j \le i} \sum_{k \le i} X_{ijk} \frac{V_j + V_k}{V_j V_k} a\left(V_j, V_k\right) f_j f_k \tag{6}$$

$$D_{ag,i} = \rho_g \alpha_g^2 \sum_{j=1}^{N} a\left(V_i, V_j\right) f_i f_j \frac{1}{V_j} \tag{7}$$

$$B_{br,i} = \rho_g \alpha_g \sum_{j>i} g\left(V_j, V_i\right) f_j \tag{8}$$

$$D_{br,i} = \rho_g \alpha_g \sum_{j<i} g\left(V_i, V_j\right) f_i \tag{9}$$

Here, $a\left(V_i, V_j\right)$ is the coalescence rate between bubbles of sizes V_i and V_j, $g\left(V_i, V_j\right)$ is the partial breakup rate of a mother bubble of size V_i which splits into a daughter bubble of size V_j and its complement, and X_{ijk} is the fraction of a bubble of size *V* formed by coalescence of bubbles of sizes V_j and V_k assigned to group *i*.

$$X_{ijk} = \begin{cases} \dfrac{V - V_{i-1}}{V_i - V_{i-1}} & \text{if} \quad V_{i-1} < V < V_i \\ \dfrac{V_{i+1} - V}{V_{i+1} - V_i} & \text{if} \quad V_i < V < V_{i+1} \\ 0 & \text{otherwise} \end{cases} \tag{10}$$

Bubbles of the smallest class do not break up; their death rate $D_{br,1}$ is therefore zero. The sum of source terms over all classes must be equal to zero to conserve mass. To close the system of equations, the models that describe the coalescence and breakup rates must be introduced; these are discussed in detail in the following text.

Coupling the population balance model (PBM) with hydrodynamics is conducted via the Sauter mean diameter (SMD). The flow field, phase fractions and turbulent quantities are calculated by CFD and are used to solve the PBM. The resulting bubble size distribution is used to calculate the SMD in each computational cell. This value of the SMD then enters the calculation of the drag coefficient and the interphase forces.

3.1.1. Bubble coalescence

The random motion of fluid particles in turbulent flows is usually assumed to be similar to the random movement of gas molecules. Hence, most of the present models for coalescence, $a\left(V_i, V_j\right)$, were

derived analogously to the classical kinetic theory of gases, where collisions between molecules are considered.

The coalescence rate is directly proportional to the collision frequency of bubbles ω_{ag}. Because the duration of collisions is limited and because coalescence will only occur if the interaction time between bubbles is sufficiently long, the concept of the collision efficiency P_{ag} is introduced. The resulting coalescence rate is then the product of these two quantities:

$$a(V_i, V_j) = \omega_{ag}(V_i, V_j) P_{ag}(V_i, V_j) \tag{11}$$

Various mechanisms of coalescence are presently known (Liao and Lucas, 2010). Most of these mechanisms are usually neglected, especially in stirred tanks with high levels of turbulence, when compared with turbulence-induced coalescence, which results from the random motion of bubbles due to turbulent fluctuations. In this work, buoyancy-driven collisions resulting from the difference in the rise velocities of bubbles having different sizes are also incorporated. The total coalescence rate is assumed to be the sum of all rates that arise from the different mechanisms.

One of the most widely used coalescence models is described by Prince and Blanch (1990). The turbulence-induced and buoyancy-driven collision frequencies $\omega_{ag,t}$ and $\omega_{ag,b}$ and the collision efficiency P_{ag}, which is supposed to be the same for both mechanisms, are expressed as:

$$\omega_{ag,t}(V_i, V_j) = F_{ag,t} \frac{\pi}{4} \sqrt{2} (d_i + d_j)^2 \varepsilon^{1/3} \left(d_i^{2/3} + d_j^{2/3}\right)^{1/2} \tag{12}$$

$$\omega_{ag,b}(V_i, V_j) = F_{ag,b} \frac{\pi}{4} (d_i + d_j)^2 \left|U_{r,j} - U_{r,i}\right| \tag{13}$$

$$P_{ag}(V_i, V_j) = \exp\left(-\frac{\rho_l^{1/2} r_{ij}^{5/6} \varepsilon^{1/3}}{4\sigma^{1/2}} \ln\frac{h_0}{h_f}\right) \tag{14}$$

where

$$U_{r,i} = \sqrt{\frac{2.14\sigma}{\rho_l d_i} + 0.505 g d_i}, \qquad r_{ij} = \left(\frac{1}{2}\left(\frac{1}{r_i} + \frac{1}{r_j}\right)\right)^{-1} \tag{15}$$

$F_{ag,t}$ and $F_{ag,b}$ are the calibration factors, σ is the surface tension, h_0 is the initial thickness of a film that separates the coalescing bubbles and h_f is the critical thickness at which the rupture of the film and coalescence occurs (10^{-4} and 10^{-8} m, respectively).

3.1.2. Bubble breakup

Bubble breakage generally depends on the balance between the external stresses that disrupt the bubble and the viscous stresses represented by the surface tension that resist bubble deformation. Most of the published breakup models are based on similar assumptions:

- Bubble breakup in a turbulent flow is caused by turbulent eddies that hit the bubble surface and so deform the bubble.
- For the breakup to occur, the eddies must have energy large enough to overcome the resisting forces.
- The eddies should be smaller or equal to the size of the bubble.
- Eddies larger than the bubble only transport the bubble.
- Only binary breakup occurs.
- The turbulence is isotropic.

- Bubble sizes are in the inertial range of turbulence.

Because of the third and fourth assumptions, the breakup rate of bubbles should decrease with their decreasing size. The breakup rate of very small bubbles is close to zero because eddies that are smaller than the bubbles do not have enough energy to break them, and larger eddies only transport these bubbles. The bubble size under which no breakup occurs is dependent on the turbulent dissipation energy: the larger the energy dissipation rate, the greater the amount of energy that is stored in turbulent eddies, and so the smaller bubbles can be broken.

As mentioned above, the coalescence models are usually derived from similar assumptions resulting from the kinetic theory of gases, and so they exhibit similar behaviours. Many breakup models, $g\left(V_i, V_j\right)$, followed the kinetic theory of gases as well. The breakup frequency is then provided by the collision rate between the particles and the turbulent eddies multiplied by the collision efficiency. However, the collision efficiency terms are based on various assumptions such as that breakup occurs if a critical value of the eddy energy (Luo and Svendsen, 1996) or the relative velocity of oscillations (Alopaeus et al., 2002) is exceeded, or if the dynamic pressure of the eddy is larger than the capillary pressure of the smaller daughter bubble (Lehr et al., 2002). Besides, models based on kinematic ideas were proposed (Martínez-Bazán et al., 1999a, b). Therefore, various breakup models significantly differ in the predicted breakup frequencies and in the shapes of the DSD functions.

The model by Luo

Luo and Svendsen (1996) proposed a kinetic theory-type model. They predicted that to induce breakup, the energy of the incoming eddy must be larger than the increase in the surface energy due to bubble breakup. The partial breakup rate is given as:

$$g\left(V_i, V_j\right) = F_{br}\, 0.9238 \frac{\varepsilon^{1/3}}{d_i^{2/3}} \left(1-\alpha_g\right) \int_{\xi_{\min}}^{1} \frac{(1+\xi)^2}{\xi^{11/3}} \exp\left(-\frac{12 c_f \sigma}{\beta \rho_l \varepsilon^{2/3} d_i^{5/3} \xi^{11/3}}\right) \mathrm{d}\xi \tag{16}$$

where ξ is the dimensionless eddy size, c_f is the coefficient of change in the surface area, β is a constant equal to 2, and F_{br} is a calibration coefficient. The total breakup frequency of bubbles of size V_i is then computed as an integral over all possible daughter bubble sizes. For more details please refer to Kálal et al. (2014).

A necessary part of each breakup model is the DSD function $\beta(1, f)$ that describes the probability of formation of a daughter particle of a volumetric fraction f of the mother particle. The DSD function must satisfy the following constraints:

$$\int_0^1 \beta(1, f)\mathrm{d}f = \nu\left(V_i\right) \tag{17}$$

$$\int_0^1 V_i \cdot f \cdot \beta(1, f)\mathrm{d}f = V_i \tag{18}$$

where $\nu\left(V_i\right)$ is the number of fragments formed by breakage of a mother particle of size V_i.

A great advantage of the model by Luo is that the DSD function is derived directly from the expression for the breakup rate and is found by normalising the partial breakup rate by the overall breakup rate.

$$\beta(1, f) = \frac{g\left(V_i, V_j\right)}{g\left(V_i\right)} \tag{19}$$

The breakup frequency and the DSD function of the model are plotted in Fig. 1. The curve of the DSD function is U-shaped, which indicates that it predicts high probabilities for breakups in small bubbles and their complements, and the lowest probability for an equal-sized breakup. This results from the surface energy change assumption: when two bubbles of the same size are formed, the increase in the surface energy is the largest and so only eddies with large energy can cause such breakup, which makes this option the least probable.

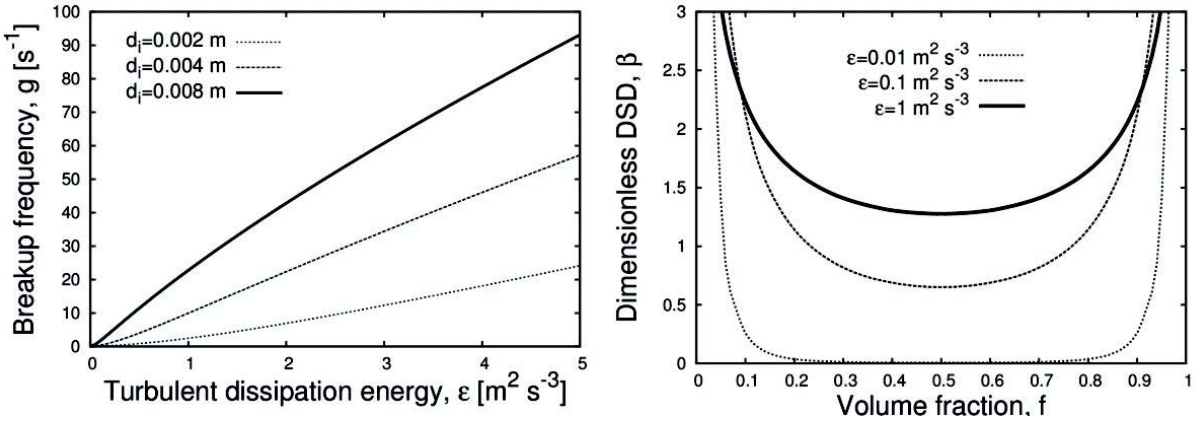

Fig. 1. Luo model ($\alpha_g = 0.01, d_i = 0.008$ m)

The model by Martínez-Bazán

Martínez-Bazán et al. (1999a, b) criticised the models that make use of questionable closures for the number density of eddies, eddy-bubble collision cross-section, etc. Therefore, they proposed a model based purely on kinematic ideas with no collision efficiency term.

The basic premise of this model is that to cause bubble breakup, the turbulent stresses produced by the surrounding liquid must be larger than the forces that hold the bubble together. The breakup frequency is then proportional to the difference between these two forces. In the following equation, the disruption and confinement forces are represented by the two terms under the square root:

$$g(V_i) = F_{br} K_g \frac{\sqrt{\beta(\varepsilon d_i)^{2/3} - 12\dfrac{\sigma}{\rho_l d_i}}}{d_i} \tag{20}$$

The probability of breakup increases with an increasing value of the difference under the square root. When the confinement forces are larger or equal to the disrupting forces, the breakup frequency is equal to zero. The values of the constants K_g and β are 0.25 and 8.2, respectively.

Unlike the previous model, the DSD function is bell-shaped and predicts the highest probability for the breakup of a mother bubble into two half-sized daughter bubbles (Fig. 2). The daughter bubbles must satisfy the condition that $d_{min} < d_j < d_{max}$, i.e., the size of the daughter bubble is restricted by the minimum and maximum values.

$$\beta(1, f) = 2 \cdot \frac{\left(f^{2/9} - \Lambda^{5/3}\right)\left[(1-f)^{2/9} - \Lambda^{5/3}\right]}{\int_{f_{min}}^{f_{max}} \left(f^{2/9} - \Lambda^{5/3}\right)\left[(1-f)^{2/9} - \Lambda^{5/3}\right] df} \tag{21}$$

where

$$f_{\min}=\frac{d_{\min}^3}{d_i^3};\quad f_{\max}=\frac{d_{\max}^3}{d_i^3};\quad \Lambda=\frac{d_c}{d_i};\quad d_c=\left(\frac{12\sigma}{\beta\rho_l}\right)^{3/5}\varepsilon^{-2/5};$$
$$d_{\min}=\left(\frac{12\sigma}{\beta\rho_l d_i}\right)^{3/2}\varepsilon^{-1};\quad d_{\max}=d_i\left[1-\left(\frac{d_{\min}}{d_i}\right)^3\right]^{1/3} \tag{22}$$

The critical diameter d_c is defined as the bubble size at which the deforming and confining forces are in balance. It applies to the mother bubble and signifies the minimum bubble size for which breakup can occur in given conditions. On the other hand, the minimum and maximum diameters d_{min} and d_{max} apply to the daughter bubbles and define the smallest and the largest bubbles that can be formed under the given conditions by the breakup of the mother bubble.

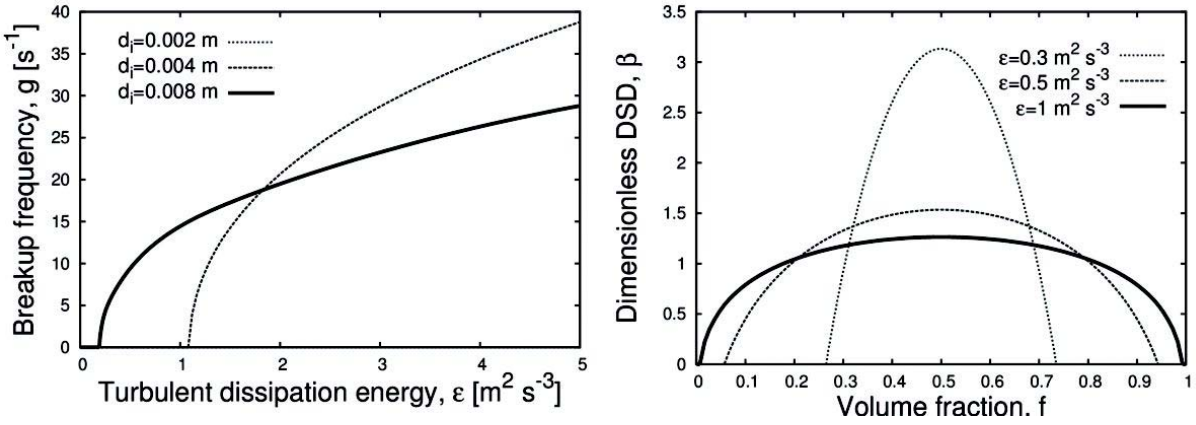

Fig. 2. Martínez-Bazán model ($d_i = 0.008$ m)

The model by Lehr

Lehr et al. (2002) based their approach on the assumption that to break up a bubble, the kinetic energy of the incoming eddy must exceed the interfacial energy of the smaller daughter bubble. This condition is sometimes called the capillary constraint. It is the dominant constraint for formation of bubbles with radius tending to zero because the interfacial force (capillary pressure) of such bubbles is very high and thus the arriving eddy may not provide enough inertial force (dynamic pressure) to overcome the capillary pressure. Breakup does not occur then even though the energy constraint based on, e.g., the surface energy change is satisfied.

As in the model described by Luo, this model provides the partial breakup frequency in an integral form. To avoid the computation of the integral, the authors provided analytical solutions of the total breakup frequency and the DSD function:

$$g(V_i)=F_{br}\,0.5\,\frac{d_i^{5/3}\varepsilon^{19/15}\rho_l^{7/5}}{\sigma^{7/5}}\exp\left(-\frac{\sqrt{2}\sigma^{9/5}}{d_i^3\rho_l^{9/5}\varepsilon^{6/5}}\right) \tag{23}$$

$$\beta(1,f)=\begin{cases}\dfrac{1}{\pi^{1/2}f}\cdot\dfrac{exp\left\{-\dfrac{9}{4}\left[ln\left(\dfrac{2^{2/5}d_j\rho_l^{3/5}\varepsilon^{2/5}}{\sigma^{3/5}}\right)\right]^2\right\}}{1+\mathrm{erf}\left[\dfrac{3}{2}ln\left(\dfrac{2^{1/15}d_i\rho_l^{3/5}\varepsilon^{2/5}}{\sigma^{3/5}}\right)\right]} & 0<f<\dfrac{1}{2}\\ \beta(1,1-f) & \dfrac{1}{2}<f<1\end{cases} \tag{24}$$

The DSD function prefers the equal-sized breakup in low-turbulence environments (Fig. 3). Small eddies do not have sufficient energy to split off small daughter bubbles from the mother bubbles; larger eddies with larger energy will more likely cause the breakup. Therefore, breakage to two equal-sized bubbles is the most probable case as is predicted by the bell-shaped DSD function. When the turbulent dissipation rate increases, the number and energy of small eddies considerably increase, which leads to breakage into one smaller and one larger bubble; however, the formation of very small bubbles is still limited by the capillary constraint. Thus, the unequal-sized breakage is preferred and the DSD function becomes M-shaped.

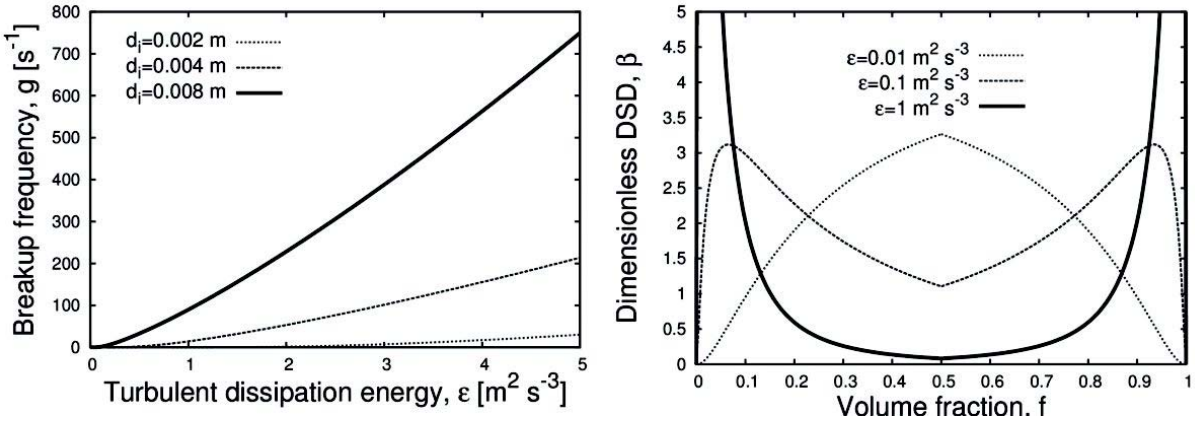

Fig. 3. Lehr model ($d_i = 0.008$ m)

The model by Alopaeus

Narsimhan et al. (1979) derived a model for liquid drop breakup. The fundamental assumption of the model is that particle oscillations are brought about by the relative velocity fluctuations between points near the vicinity of the droplet surface, which causes an increase in the surface energy. If a minimum relative velocity of oscillations and so a minimum increase in the surface energy needed for fragmentation are exceeded, breakup occurs.

Alopaeus et al. (2002) modified the expression by Narsimhan et al. (1979) by adding a dependency of the drop-eddy collision frequency on the turbulent dissipation energy and by including viscous forces of the dispersed phase as resisting forces. Laakkonen et al. (2007) used this kernel to describe bubble breakup. They further modified the expression by replacing the dispersed phase viscosity with the continuous phase viscosity because viscous stresses that resist the breakage are assumed to be proportional to the viscosity of the liquid surrounding the bubble rather than the viscosity of gas, which is small:

$$g(V_i) = F_{br}\varepsilon^{1/3}\mathrm{erfc}\left(\sqrt{C_1\frac{\sigma}{\rho_l\varepsilon^{2/3}d_i^{5/3}} + C_2\frac{\mu_l}{\sqrt{\rho_l\rho_g}\varepsilon^{1/3}d_i^{4/3}}}\right) \tag{25}$$

Values of the constants C_1 and C_2 for the gas-liquid stirred tanks were proposed by Laakkonen et al. (2007) to be 0.04 and 0.01, respectively. A $d^{-2/3}$ dependence would make the parameter F_{br} dimensionless. However, such dependence would lead to a decrease in the breakup frequency with increasing bubble diameter, which is not physically acceptable.

The authors did not derive any corresponding DSD function. Instead, they used a simple, statistical function, namely a β-distribution. In contrast to the previous elaborated, phenomenological DSD functions, the β-distributions are dependent only on the sizes of the mother and daughter bubbles and not on the physical properties of the system. In this work, the following formula was used (Fig. 4):

$$\beta(1, f) = 60 \cdot f^2 (1 - f)^2 \tag{26}$$

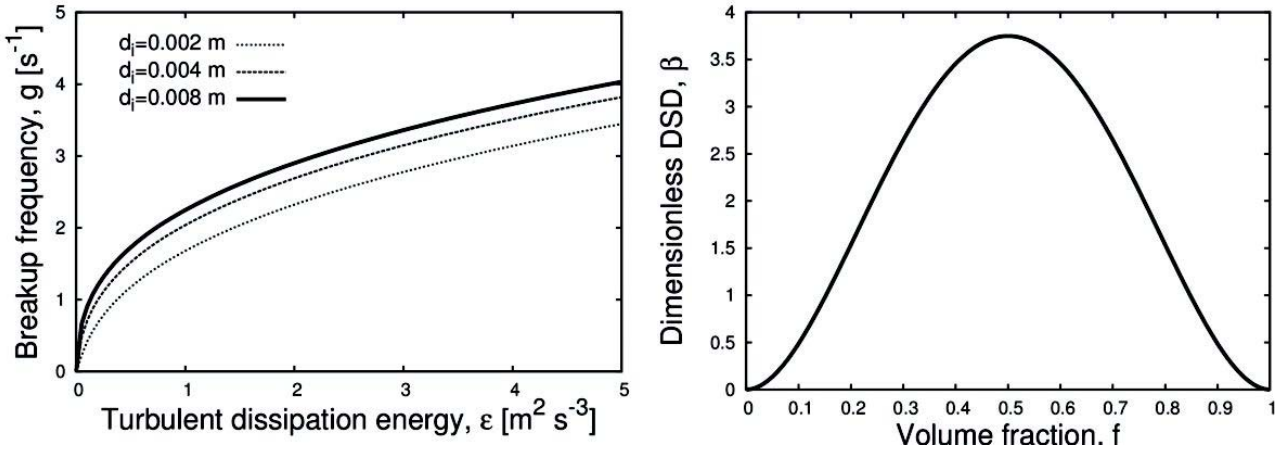

Fig. 4. Alopaeus model ($d_i = 0.008$ m)

Most breakup models do not have an expression for the partial breakup frequency that appears in the equations of MUSIG model (Eqs. (7), (8)). However, it can be derived from Eq. (18) as the product of the overall breakup frequency and the DSD function.

In this part, we described only four breakup models that were used in our simulation studies. Exhausting reviews on the breakup frequency and DSD function models were presented by Lasheras et al. (2002) and Liao and Lucas (2009).

4. COMPUTATIONAL DOMAIN AND NUMERICAL TECHNIQUES

Four structured computational grids ranging from 185 000 cells to 3.5 million cells were tested on the investigated system. The finest grid underestimated the power number computed from the overall dissipation energy by approximately 18% in comparison with the correlation given by Rutherford et al. (1996), while the error of the coarsest grid was nearly 60%. Because the improvement in the turbulent field prediction for very fine grids is quite slow, a two-million mesh was chosen for further computations. It gave nearly the same results as the finest grid while the computational time was halved.

CFD simulations were performed using the software CFX 14.5. The standard *k-ε* turbulence model was used, and the impeller motion was modelled using the MRF (Multiple Reference Frames) method. The PBE was solved using the MUSIG method with 24 bubble size groups in the range from 0.5 to 16 mm. The drag coefficient correlation and breakup models were implemented in the solver through user-defined functions.

The second order upwind discretisation scheme was adopted for the convective terms of the governing equations. A substantial under-relaxing was applied in the pseudo-steady-state simulations. This ensured, in combination with the fully implicit solver, smooth convergence to final solution. At the end of every simulation the residuals of all variables were well below 10^{-4}. Besides, the global gas hold-up in the system was monitored and the pseudo-steady-state was assumed to be achieved when this quantity remained constant. More details about the grid-sensitivity tests and numerical settings can be found in Kálal et al. (2014).

5. RESULTS AND DISCUSSION

On the basis of experiments, the global gas hold-up in the system was found to be equal to (0.70 ± 0.04) and (1.10 ± 0.05) vol.% for the investigated gas flow rates (0.2 and 0.4 vvm, respectively). Qualitative evaluation of the local gas hold-up was performed on the basis of visual observation.

Large bubbles injected in the system from the sparger enter the high-turbulent impeller region, which causes an intensive breakup of the bubbles and results in a low value of the SMD. The bubble diameter then slowly increases in the axial direction from the impeller plane towards the liquid surface and in a radial direction from the vessel wall towards the shaft. Obviously, coalescence prevails in the volume above the impeller plane. The smallest SMD was observed in position A under the impeller because the system was working in the loading regime when the vast majority of bubbles followed the upper recirculation loops and only the small bubbles were captured by the lower loops. Both the local SMDs and volume-based BSDs were obtained from the experiments and calculated using all investigated models and are compared in Figs. 5 – 8.

All breakup models were adjusted by setting the calibration coefficient F_{br} so that the measured and modelled SMDs were coincident at the outflow from the impeller in area B. Attention was then focused on the ability of the models to describe the evolution of the SMD and the shape of the BSD throughout the tank. The model by Luo and Svendsen (1996) predicted the SMDs quite well at points A-D along the wall, but in the bulk of the system the model was not able to compensate the coalescence and the resulting diameters were overpredicted. We note that in Kálal et al. (2014) we had achieved a good agreement between the experimental and numerical values of the SMD for this model throughout the whole tank under nearly the same model setting. The only difference had been that the buoyancy-driven coalescence had not been included. Now it was obviously responsible for the increase in the bubble sizes in the bulk. This suggests that the successful prediction of the SMD is dependent on the correct assessment which bubble size change mechanisms to include in the model. Before we present the BSDs, we have to discuss some important features of the model.

The DSD function of the Luo's model is U-shaped (Fig. 1). It predicts the highest probability for breakup in an infinitely small bubble and its complement, which is nearly as large as the original mother bubble. According to the theory by Luo & Svendsen, breakup occurs whenever the energy of the incoming eddy is higher than the change in the surface energy due to bubble breakup, i.e., the breakup should occur whenever a bubble is hit by an eddy because a formation of an infinitely small bubble and its complement causes an infinitely small change in the surface energy and thus requires infinitely small energy to be contained in the eddy. However, this behaviour is not correct. For breakups with small daughter/mother bubble volume ratios, the capillary pressure is high and even an eddy with a large kinetic energy may not produce enough dynamic pressure to overcome the capillary pressure (Wang et al., 2003). So, in reality, the size of the daughter bubble has a minimum due to the capillary pressure and a maximum due to the increase in the surface energy.

The described shortcoming gives rise to the sensitivity of the model to the discretisation of the bubble population, namely to the size of the smallest bubble group, which was described in Kálal et al. (2014). The results presented in Figs. 5 – 8 were obtained using a minimum bubble size $d_{b,min}$ = 0.5 and the calibration coefficient F_{br} = 0.12. When we changed the minimum bubble size to 0.1 mm, nearly all bubbles were completely smashed into very small bubbles with diameters close to the size of this smallest group. This behaviour stems from the discussed shortcoming of the model – when we decreased the minimum bubble size, we decreased the energy that is needed to bring about the breakup into the smallest bubbles and so smaller eddies with lower energy were able to pinch off these smallest daughter bubbles. After each breakup, a very small bubble and its complement were produced. The complement remained nearly as large as the original mother bubble and maintained a high breakup

frequency. In the end, a large number of bubbles of the smallest size was created. The resulting SMD varied with the change in the minimum bubble size. Therefore, it was necessary to adjust not only the calibration coefficient of the breakup model but also the minimum bubble size.

The BSDs corresponded to the theory. Very small bubbles (less than 1 mm) contained more gas volume than according to the experiments. We note that although these very small bubbles may contain only a small fraction of the total gas volume, they contain a large interfacial area and thus can have an important influence on the predicted SMDs. We also observed a peak at approximately 8 mm, i.e., the size of bubbles entering the system. This confirms the idea that the small bubbles are gradually peeled off these large bubbles, which remain nearly as large as they were at the entrance of the system. When they leave the impeller discharge stream, they coalesce again and the peak becomes more pronounced. Generally, the predicted BSDs are very wide and flat and do not correspond to the experimental data.

In spite of all the limitations that make the real predictivity of the model by Luo questionable, it has been the most frequently used breakup model in recent years. It has been applied by many authors for modelling the BSD in stirred tanks. However, the use of different breakup models should be obviously considered. Wang et al. (2003) proposed a modification of the Luo model by including the capillary constraint. The resulting DSD function is M-shaped and so prevents the formation of unreasonably small bubbles. Although the model might have good potential, the expression for the breakup frequency contains a double integral and the DSD function includes even a triple integral, which makes the model unfeasible for CFD simulations.

The model by Martínez-Bazán et al. (1999a, b) showed an overprediction of the SMD throughout the domain. Notice that the predicted breakup frequency of small bubbles is zero even under high turbulence levels and middle-sized bubbles still break up only at $\varepsilon > 1.0\,\mathrm{m^2/s^3}$ (Fig. 2). In other words, a high turbulence intensity is required for breakup to occur, and so nearly all breakup takes place in the vicinity of the impeller. The bubble breakup in the bulk of the system is almost absent because the predicted confinement forces are larger than the disrupting forces (Eq.(19)), which results in a zero breakup frequency. The change of bubble size in the bulk is thus controlled almost only by coalescence and the SMDs tend to be overestimated. Besides, the model predicts a smaller breakup rate for large bubbles than for smaller bubbles above a certain level of turbulence, which does not correspond to reality. The simulated BSDs captured the single-peaked shape correctly, but contained too few small bubbles. The breakup coefficient was set to $F_{br} = 0.75$.

As in the previous case, the model by Lehr et al. (2002) similarly overpredicted the SMD in the system. The reason is clear from inspection of the expression for the breakup frequency. It is strongly dependent on the turbulent dissipation energy and the mother bubble diameter. For large values of these quantities, the values of the breakup frequency are larger by one or two orders in comparison with the other breakup models (see Fig. 3). The predicted breakup frequency in the impeller discharge stream is therefore very high. On the contrary, the bubble breakup in the bulk of the system is basically non-existent because the predicted breakup frequency is nearly zero under the local conditions. As a result, breakup occurs only in the impeller plane and the bubble size change in other parts of the domain is driven by nearly pure coalescence. Because the value of the turbulent dissipation energy is high in the impeller plane, the DSD function is sharply M-shaped with high probabilities for the formation of a small daughter bubble and its complement and a nearly zero-probability of equal-sized breakup. That is why the computed BSDs are significantly bimodal with two peaks located at the bubble sizes corresponding to small bubbles and to the bubbles entering the system. The breakup coefficient was set to $F_{br} = 0.004$.

Martínez-Bazán et al. (1999a, b) derived their model for a submerged water jet, whereas Lehr et al. (2002) derived and validated the model for bubble columns. However, our results show that these models are not appropriate for BSD modelling in much more turbulently inhomogeneous systems like

stirred tanks. This suggests that the validity and transferability of the available breakup models is limited.

In contrast with Lehr's model, the model by Alopaeus et al. (2002) shows a much weaker dependence of the breakup frequency on the mother bubble size and turbulent dissipation energy (Fig. 4). This resulted in the fact that the breakup model was able to compensate the coalescence in the bulk of the system and the predicted SMDs throughout the tank were in good agreement with the experimental values, except at location A, where the deviation was likely caused by an underestimated local gas hold-up. The simulated BSDs predicted the single peak correctly, but contained longer tails than the measured curves. While the numerical results suggest that large bubbles contain a considerable amount of gas, the maximum bubble size observed during photographic measurements was approximately 6 mm. The reason for this discrepancy was probably that during experiments we evaluated only 300-600 bubbles for each measurement point at each gas flow rate, which may not be a statistically significant number of bubbles. The number density of small bubbles is much larger than that of large bubbles so if more photographs were evaluated, very large bubbles might be found. The volume-based BSDs can be influenced substantially even by one large bubble, e.g., one bubble of 10 mm contains the same amount of gas as 1000 bubbles of size of 1 mm. Obviously, thousands of bubbles would have to be evaluated to obtain a fully representative volume-based BSDs. A shortcoming in the mathematical model is another explanation for why the long tails are formed. The breakup coefficient was set to $F_{br} = 7$. The bell-shaped DSD function favours the equal-sized breakup. Despite the fact that it is not consistent with the surface energy change consideration, it is mathematically more convenient compared with the U-shaped or M-shaped models. The probability of formation of very small bubbles approaches zero while the size of the smallest bubble group decreases; hence, the model is not sensitive to the change of the minimum bubble size as it is in the case of Luo's model.

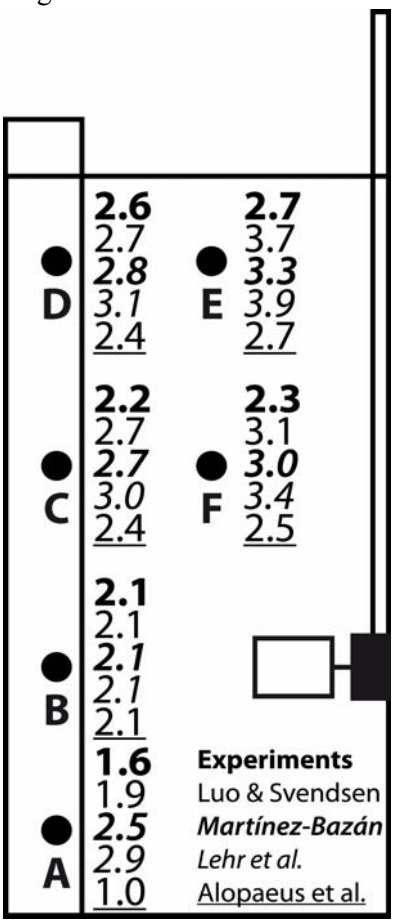

Fig. 5. Sauter mean diameters at the investigated locations obtained both experimentally and numerically via various breakup models, $Q = 0.2$ vvm, $N = 300$ rpm

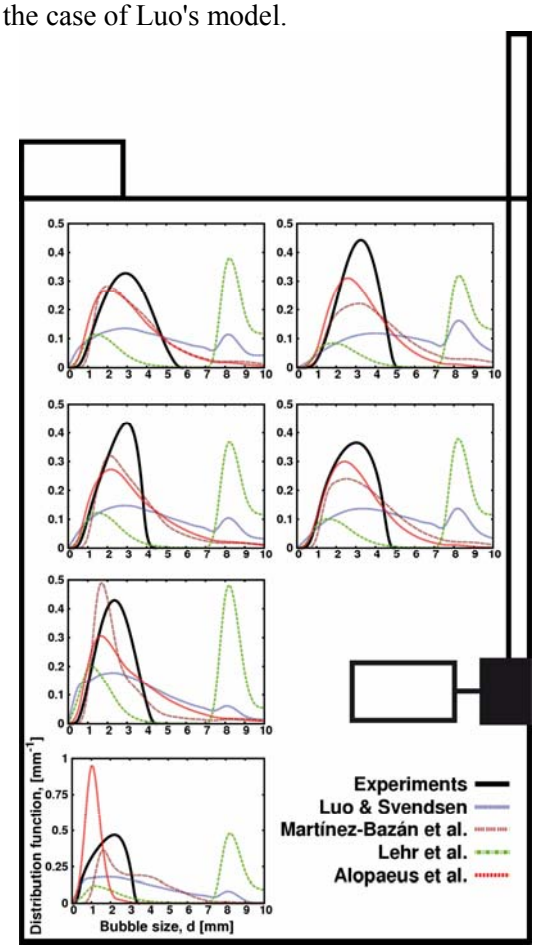

Fig. 6. Bubble size distributions at the investigated locations obtained both experimentally and numerically via various breakup models, $Q = 0.2$ vvm, $N = 300$ rpm

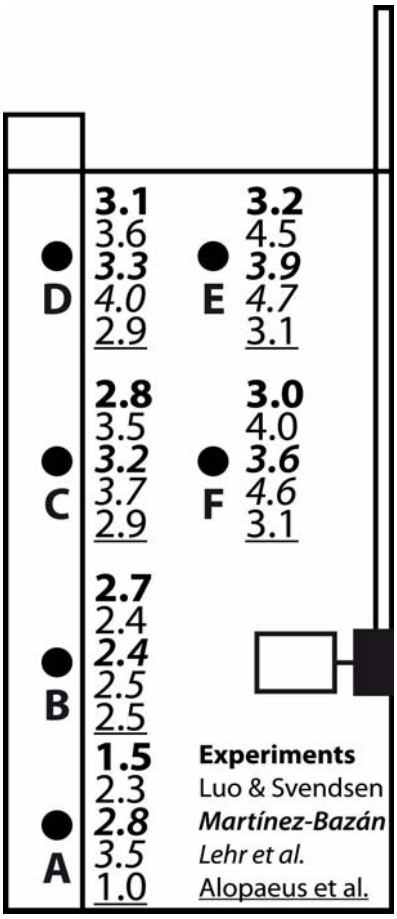

Fig. 7. Sauter mean diameters at the investigated locations obtained both experimentally and numerically via various breakup models, $Q = 0.4$ vvm, $N = 300$ rpm

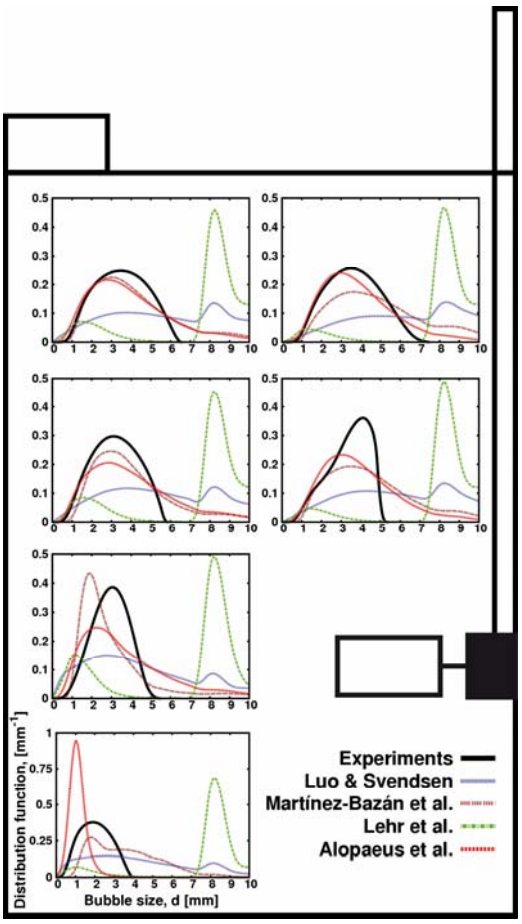

Fig. 8. Bubble size distributions at the investigated locations obtained both experimentally and numerically via various breakup models, $Q = 0.4$ vvm, $N = 300$ rpm

6. CONCLUSIONS

In this work, the bubble size distribution in an aerated stirred tank was modelled using several different breakup models and the computed local SMDs and BSDs were compared with experimental results. The model by Luo overpredicted the bubble sizes in the bulk of the system. As a result of the daughter size distribution function of the model, the BSDs contained too many very small bubbles and too many large bubbles, making the distribution flat without a significant peak. Because of the sensitivity to the size of the smallest bubble group, the model must be adjusted using experimental data and thus its general applicability is questionable. Both the model by Martínez-Bazán and that by Lehr overpredicted the SMDs in the system. While the former model was able to describe the single-peak shape of the BSDs correctly, the latter predicted bimodal distributions. By contrast, the model by Alopaeus was able to predict the bubble sizes well throughout the tank and the BSDs captured the single peak in agreement with experimental data. Although all models were adjusted to predict the same SMD at the point B at the outflow from the impeller, the resulting BSDs were completely different. This suggests that the shape of the distributions should be brought into focus because the BSDs have been usually either neglected or presented without comparison with experimental data, and only SMDs have been compared.

This project has been supported by the Czech Science Foundation (Grant: 104/09/1290) and by specific university research (Grant: MSMT No 20/2013).

SYMBOLS

$a(V_i, V_j)$	coalescence rate, $m^3\ s^{-1}$
$B(V,t)$	birth rate of bubbles, $m^{-6}\ s^{-1}$
B_i	birth rate of bubbles in class *i*, $m^{-3}\ s^{-1}$
c_D	drag coefficient
c_f	change in the surface area
d	diameter, m
$D(V,t)$	death rate of bubbles, $m^{-6}\ s^{-1}$
D_i	death rate of bubbles in class *i*, $m^{-3}\ s^{-1}$
F_{ag}, F_{br}	calibration coefficients
f	daughter/mother bubble volume ratio
f_i	volumetric fraction of class *i* in gas phase
$g(V_i)$	overall breakup rate, s^{-1}
$g(V_i, V_j)$	partial breakup rate, s^{-1}
h_0, h_f	initial, critical thickness of the liquid film separating bubbles, m
$n(V,t)$	bubble number density function, m^{-6}
n_i	number of bubbles per unit volume, m^{-3}
P_{ag}	collision efficiency
Q	gas flow rate, $m^3\ s^{-1}$
r	radius, m
T	mixing vessel diameter, m
$\vec{U}$	average velocities vector, $m\ s^{-1}$
U_s	terminal rise velocity in stagnant fluid, m s-1
U_t	terminal rise velocity in turbulent fluid, $m\ s^{-1}$
V	volume, m^3
X_{ijk}	fraction of a bubble (Eq.(9))

Greek symbols

α	volume fraction
$\beta(1,f)$	dimensionless daughter size distribution function
ε	turbulent dissipation energy, $m^2\ s^{-3}$
η	Kolmogorov microscale, m
μ	dynamic viscosity, Pa s
ν	number of fragments formed by breakup
ξ	dimensionless eddy size
ρ	density, $kg\ m^{-3}$
σ	surface tension, $N\ m^{-1}$
ω_{ag}	collision frequency, $m^3\ s^{-1}$

Subscripts

ag, br	aggregation, breakup
b	bubble
g, l	gas, liquid phase
i, j, k	index of a bubble size group

REFERENCES

Ahmed S. U., Ranganathan P., Pandey A., Sivaraman S., 2010. Computational fluid dynamics modeling of gas dispersion in multi impeller bioreactor. *J. Biosci. Bioeng.*, 109, 588-597. DOI: 10.1016/j.jbiosc.2009.11.014.

Alopaeus V., Koskinen J., Keskinen K.I., Majander J., 2002. Simulation of the population balances for liquid-liquid systems in a nonideal stirred tank. Part 2 - parameter fitting and the use of the multiblock model for dense dispersions. *Chem. Eng. Sci.*, 57, 1815-1825. DOI: 10.1016/S0009-2509(02)00067-2.

Alves S.S., Maia C.I., Vasconcelos J.M.T., 2002. Experimental and modelling study of gas dispersion in a double turbine stirred tank. *Chem. Eng. Sci.*, 57, 487-496. DOI: 10.1016/S0009-2509(01)00400-6.

Andersson R., Andersson B., 2006. On the breakup of fluid particles in turbulent flows. *AIChE J.*, 52, 2020-2030. DOI: 10.1002/aic.10831.

Bakker A., van den Akker H.E.A., 1994. A computational model for the gas-liquid flow in stirred reactors. *Chem. Eng. Res. Des.*, 72, 594-606.

Clift R., Grace J.R., Weber M.E., 1978. *Bubbles, drops, and particles*. Academic Press, New York, USA.

Coroneo M., Montante G., Paglianti A., Magelli F., 2011. CFD prediction of fluid flow and mixing in stirred tanks: Numerical issues about the RANS simulations. *Comput. Chem. Eng.*, 35, 1959-1968. DOI: 10.1016/j.compchemeng.2010.12.007.

Fajner D., Pinelli D., Ghadge R. S., Montante G., Paglianti A., Magelli F., 2008. Solids distribution and rising velocity of buoyant solid particles in a vessel stirred with multiple impellers. *Chem. Eng. Sci.*, 63, 5876-5882. DOI: 10.1016/j.ces.2008.08.033.

Gimbun J., Rielly C.D., Nagy Z.K., 2009. Modelling of mass transfer in gas-liquid stirred tanks agitated by Rushton turbine and CD-6 impeller: A scale-up study. *Chem. Eng. Res. Des.*, 87, 437-451. DOI: 10.1016/j.cherd.2008.12.017.

Gordon R.G., 1968. Error bounds in equilibrium statistical mechanics. *J. Math. Phys.*, 9, 655-663. DOI: 10.1063/1.1664624.

Hesketh R.P., Etchells A.W., Russell T.W.F., 1991. Experimental observations of bubble breakage in turbulent flow. *Ind. Eng. Chem. Res.*, 30, 835-841, DOI: 10.1021/ie00053a005.

Kálal Z., Jahoda M., Fořt I., 2014. CFD prediction of gas-liquid flow in an aerated stirred vessel using the population balance model. *Chem. Process Eng.*, 35, 55-73. DOI: 10.2478/cpe-2014-0005.

Kerdouss F., Bannari A., Proulx P., Bannari R., Skrga M., Labrecque Y., 2008. Two-phase mass transfer coefficient prediction in stirred vessel with a CFD model. *Comput. Chem. Eng.*, 32, 1943-1955. DOI: 10.1016/j.compchemeng.2007.10.010.

Khopkar A.R., Rammohan A.R., Ranade V.V., Dudukovic M.P., 2005. Gas-liquid flow generated by a Rushton turbine in stirred vessel: CARPT/CT measurements and CFD simulations. *Chem. Eng. Sci.*, 60, 2215-2229. DOI: 10.1016/j.ces.2004.11.044.

Kumar S., Ramkrishna D., 1996. On the solution of population balance equations by discretization - I. A fixed pivot technique. *Chem. Eng. Sci.*, 51, 1311-1332. DOI: 10.1016/0009-2509(96)88489-2.

Laakkonen M., Moilanen P., Alopaeus V., Aittamaa J., 2007. Modelling local bubble size distributions in agitated vessels. *Chem. Eng. Sci.*, 62, 721-740. DOI: 10.1016/j.ces.2006.10.006.

Lasheras J.C., Eastwood C., Martínez-Bazán C., Montanes J.L., 2002. A review of statistical models for the break-up of an immiscible fluid immersed into a fully developed turbulent flow. *Int. J. Multi. Flow*, 28, 247-278. DOI: 10.1016/S0301-9322(01)00046-5.

Lehr F., Millies M., Mewes D., 2002. Bubble-size distributions and flow fields in bubble columns. *AIChE J.*, 48, 2426-2443. DOI: 10.1002/aic.690481103.

Liao Y., Lucas D., 2009. A literature review of theoretical models for drop and bubble breakup in turbulent dispersions. *Chem. Eng. Sci.*, 64, 3389-3406. DOI: 10.1016/j.ces.2009.04.026.

Liao Y., Lucas D., 2010. A literature review on mechanisms and models for the coalescence process of fluid particles. *Chem. Eng. Sci.*, 65, 2851-2864. DOI: 10.1016/j.ces.2010.02.020.

Lo S., 1996. *Application of the MUSIG model to bubbly flows*. AEAT-1096, AEA Technology.

Luo H., Svendsen H.F., 1996. Theoretical model for drop and bubble breakup in turbulent dispersions. *AIChE J.*, 42, 1225-1233. DOI: 10.1002/aic.690420505.

Marchisio D.L., Fox R.O., 2005. Solution of population balance equations using the direct quadrature method of moments, *J. Aerosol Sci.*, 36, 43-73. DOI: 10.1016/j.jaerosci.2004.07.009.

Marchisio D.L., Fox R.O., 2013. *Computational models for polydisperse particulate and multiphase systems*. Cambridge University Press, New York, USA.

Martínez-Bazán C., Montanes J.L., Lasheras J.C., 1999a. On the breakup of an air bubble injected into fully developed turbulent flow. Part 1. Breakup frequency. *J. Fluid Mech.*, 401, 157-182. DOI: 10.1017/S0022112099006680.

Martínez-Bazán C., Montanes J.L., Lasheras J.C., 1999b. On the breakup of an air bubble injected into fully developed turbulent flow. Part 2. Size PDF of the resulting daughter bubbles. *J. Fluid Mech.*, 401, 183-207. DOI: 10.1017/S0022112099006692.

McGraw R., 1997. Description of aerosol dynamics by the quadrature method of moments. *Aerosol Sci. Tech.*, 27, 255-265. DOI: 10.1080/02786829708965471.

Mendelson H.D., 1967. The prediction of bubble terminal velocities from wave theory. *AIChE J.*, 13, 250-253. DOI: 10.1002/aic.690130213.

Montante G., Horn D., Paglianti A., 2008. Gas-liquid flow and bubble size distribution in stirred tanks. *Chem. Eng. Sci.*, 63, 2107-2118. DOI: 10.1016/j.ces.2008.01.005.

Montante G., Paglianti A., Magelli F., 2007. Experimental analysis and computational modelling of gas-liquid stirred vessels. *Chem. Eng. Res. Des.*, 85, 647-653. DOI: 10.1205/cherd06141.

Narsimhan G., Gupta J.P., Ramkrishna D., 1979. A model for transitional breakage probability of droplets in agitated lean liquid-liquid dispersions. *Chem. Eng. Sci.*, 34, 257-265. DOI: 10.1016/0009-2509(79)87013-X.

Prince M.J., Blanch H.W., 1990. Bubble coalescence and break-up in air-sparged bubble columns. *AIChE J.,* 36, 1485-1499. DOI: 10.1002/aic.690361004.

Ranganathan P., Sivaraman S., 2011. Investigations on hydrodynamics and mass transfer in gas–liquid stirred reactor using computational fluid dynamics. *Chem. Eng. Sci.*, 66, 3108-3124. DOI: 10.1016/j.ces.2011.03.007.

Rhie C.M., Chow W.L., 1983. Numerical study of the turbulent flow past an airfoil with trailing edge separation. *AIAA J.*, 21, 1525-1532. DOI: 10.2514/3.8284.

Risso F., Fabre J., 1998. Oscillations and breakup of a bubble immersed in a turbulent field. *J. Fluid Mech.*, 372, 323-355. DOI: 10.1017/S0022112098002705.

Rutherford K., Mahmoudi S M.S., Lee K.C., Yianneskis M., 1996. The influence of Rushton impeller blade and disk thickness on the mixing characteristics of stirred vessels. *Chem. Eng. Res. Des.*, 74, 369-378.

Scargiali F., D'Orazio A., Grisafi F., Brucato A., 2007. Modelling and simulation of gas-liquid hydrodynamics in mechanically stirred tanks. *Chem. Eng. Res. Des.*, 85, 637-646. DOI: 10.1205/cherd06243.

Selma B., Bannari R., Proulx P., 2010. Simulation of bubbly flows: Comparison between direct quadrature method of moments (DQMOM) and method of classes (CM). *Chem. Eng. Sci.*, 65, 1925-1941. DOI: 10.1016/j.ces.2009.11.018.

Vanni M., 2000. Approximate population balance equations for aggregation-breakage processes. *J. Coll. Int. Sci.*, 221, 143-160. DOI: 10.1006/jcis.1999.6571.

Wang T., Wang J., Jin Y., 2003. A novel theoretical breakup kernel function for bubbles/droplets in a turbulent flow. *Chem. Eng. Sci.*, 58, 4629-4637. DOI: 10.1016/j.ces.2003.07.009.

Yuan C., Fox R.O., 2011. Conditional quadrature method of moments for kinetic equations. *J. Comp. Phys.*, 230, 8216-8246. DOI: 10.1016/j.jcp.2011.07.020.

Received 30 January 2014
Received in revised form 08 May 2014
Accepted 30 May 2014